

1                   **P-NEXFS Analysis of Aerosol Phosphorus Delivered to the Mediterranean Sea**

2                   Amelia F. Longo<sup>1</sup>, Ellery D. Ingall<sup>1\*</sup>, Julia M. Diaz<sup>1§</sup>, Michelle Oakes<sup>1‡</sup>, Laura E. King<sup>1</sup>,  
3                   Athanasios Nenes<sup>2,3</sup>, Nikolaos Mihalopoulos<sup>3,4</sup>, Kaliopi Violaki<sup>4</sup>, Anna Avila<sup>5</sup>, Claudia R.  
4                   Benitez-Nelson<sup>6</sup>, Jay Brandes<sup>7</sup>, Ian McNulty<sup>8</sup> and David J. Vine<sup>8</sup>

5                   <sup>1</sup>School of Earth and Atmospheric Sciences, Georgia Institute of Technology, 311 Ferst Drive,  
6                   Atlanta, GA 30332-0340, USA.

7                   <sup>2</sup>School of Chemical and Biomolecular Engineering, Georgia Institute of Technology, 311 Ferst  
8                   Drive, Atlanta, GA 30332-0340, USA.

9                   <sup>3</sup>Foundation for Research and Technology, Hellass, Patras 70013, Greece.

10                   <sup>4</sup>University of Crete, Department of Chemistry, Iraklion 71003, Greece.

11                   <sup>5</sup>CREAF, Universitat Autònoma de Barcelona, Bellaterra 08193, Spain.

12                   <sup>6</sup>Department of Earth & Ocean Sciences & Marine Science Program, University of South  
13                   Carolina, Columbia, SC 29208, USA.

14                   <sup>7</sup>Skidaway Institute of Oceanography, 10 Ocean Science Circle, Savannah, GA 31411, USA.

15                   <sup>8</sup>Advanced Photon Source, Argonne National Laboratory, 9700 S. Cass Avenue, Argonne, IL  
16                   60439, USA.

17                   <sup>§</sup>Present address: Biology Department, Woods Hole Oceanographic Institution, Woods Hole,  
18                   MA 02543, USA.

19                   <sup>‡</sup>Present Address: Environmental Protection Agency, National Center of Environmental  
20                   Assessment, Research Triangle Park, NC 27711, USA.

21                   \*Correspondence to: ingall@eas.gatech.edu

22                   School of Earth and Atmospheric Sciences, Georgia Institute of Technology, 311 Ferst Drive,  
23                   Atlanta, GA 30332-0340, USA

24

25 **Key Points**

26     • Synchrotron-based techniques are effective tools for characterizing aerosols  
27     • Phosphorus in European and North African air masses is compositionally distinct  
28     • European aerosols deliver substantial soluble phosphorus to the Mediterranean

29 **Keywords**

30 Mediterranean, phosphorus, aerosol

31 **Abstract** Biological productivity in many ocean regions is controlled by the availability of the  
32 nutrient phosphorus. In the Mediterranean aerosol deposition is a key source of phosphorus and  
33 understanding its composition is critical for determining its potential bioavailability. Aerosol  
34 phosphorus was investigated in European and North African air masses using Phosphorus Near  
35 Edge X-ray Fluorescence Spectroscopy (P-NEXFS). These air masses are the main source of  
36 aerosol deposition to the Mediterranean Sea. We show that aerosols originating in Europe  
37 represent a significant source of soluble phosphorus to the Mediterranean. European aerosols  
38 deliver on average 3.5 times more soluble phosphorus than North African aerosols and  
39 furthermore are dominated by organic phosphorus compounds. The ultimate source of organic  
40 phosphorus does not stem from common primary emission sources. Rather, phosphorus  
41 associated with bacteria best explains the presence of organic phosphorus in Mediterranean  
42 aerosols.

43 **Index Terms**

44 Composition of aerosols and dust particles, aerosols and particles, nutrients and nutrient cycling,  
45 major and trace element geochemistry

46

47

48 **1. Introduction**

49 Atmospheric deposition is an important source of nutrients to oligotrophic ocean regions  
50 [*Graham and Duce, 1982; Mahowald et al., 2008*]. In the Eastern Mediterranean Sea, biological  
51 productivity is strongly limited by the vital nutrient phosphorus [*Krom et al., 2010; Krom et al.,*  
52 *1991*], with aerosol deposition accounting for at least one third of all phosphorus inputs [*Ganor*  
53 *and Mamane, 1982*]. Large dust plumes, clearly visible in satellite images, stretch from North  
54 Africa to the Mediterranean Sea. Perhaps as a consequence of this visible and obviously  
55 significant contribution, previous studies have focused on this region as a source of nutrients to  
56 the Mediterranean [*Escudero et al., 2011; Ganor and Mamane, 1982; Guerzoni et al.,*  
57 *1999*]. Despite the eastern Mediterranean basin receiving air masses from Europe at least 70% of  
58 the time [*Kouvarakis et al., 2001*], phosphorus supplied to the Mediterranean by European-  
59 sourced aerosols has not been as extensively studied due to comparatively lower mass  
60 deposition. Yet, it is the composition of the aerosol and the ability of microorganisms to  
61 assimilate nutrients from this source, i.e. bioavailability that must also be considered.

62 Phosphorus bioavailability has traditionally been linked to the composition and  
63 abundance of different chemical phases [*Beauchemin et al., 2003; Mackey et al., 2012*].  
64 Phosphorus is thought to be bioavailable when present as highly soluble inorganic compounds as  
65 well as simple organic molecules. Assessments of phosphorus bioavailability in aerosols have  
66 been challenged by current analytical limitations. Typically, studies of aerosol phosphorus rely  
67 upon sequential chemical extraction or leaching techniques to assess the composition, and  
68 therefore the potential bioavailability of phosphorus [*Anderson et al., 2010; Chen et al., 2006;*  
69 *Izquierdo et al., 2012; Markaki et al., 2003; Ridame and Guieu, 2002*]. These techniques have  
70 painted a complex picture of aerosol phosphorus composition, showing that phosphorus occurs

71 in a number of different phases including organic, inorganic, and mineral forms and that these  
72 phases can undergo many transformations in response to environmental conditions [Anderson *et*  
73 *al.*, 2010; Baker *et al.*, 2006; Chen *et al.*, 2006; Nenes *et al.*, 2011]; however, phases used to  
74 calibrate extraction methods were developed for soil and marine sediment analysis, thus may not  
75 be entirely representative of phosphorus phases found in aerosol. Here we combine novel  
76 synchrotron-based techniques with traditional analyses to show that European aerosols contribute  
77 phosphorus to the Mediterranean Sea that is vastly different in phosphorus composition and  
78 solubility than North African aerosols.

79 **2. Methods**

80 **2.1 Ambient aerosol collection**

81 Air masses originating in North Africa and Europe were sampled at the Finokalia research  
82 station (35°32'N, 25°67'E), a remote site on the island of Crete, Greece, located 70 km from the  
83 nearest major city. The Finokalia research station was chosen to be as far away from any local or  
84 regional influences as possible [Markaki *et al.*, 2003]. This makes the samples most  
85 representative of long range transport. Samples of particulate matter with an aerodynamic  
86 diameter of less than 10  $\mu\text{m}$ , PM10, were collected on Teflon filters using a virtual impactor with  
87 an operational flow rate of 16.7  $\text{L min}^{-1}$ . Samples were collected over a one to three day period  
88 while either North African or European air masses dominated from 2009 – 2011 (Table S1). A  
89 total of fourteen samples were analyzed, five from European air masses and nine from North  
90 African air masses (Table S1), hereafter referred to as simply European and North African  
91 samples. Hybrid Single Particle Lagrangian Integrated Trajectory Model (HYSPLIT) [Draxier  
92 and Hess, 1998; Izquierdo *et al.*, 2012] back trajectories were completed for each sample in order  
93 to confirm the geographic origin of the air masses sampled. HYSPLIT back trajectories were

94 calculated between 1000 m and 3000 m above ground level for five days preceding sample  
95 collection (Figure S1). HYSPLIT back trajectories were computed at 3000 m to check for dust  
96 events. Dust is either homogeneously distributed from 0 to about 3000 m, during spring and  
97 autumn, or is found in a layer between 2500 -4000 m during summer and  
98 autumn[Kalivitis *et al.*, 2007]. HYSPLIT back trajectories computed at 1000m show the  
99 origin of air masses within the boundary layer; this height is chosen, over 0 m or  
100 500 m, to avoid orographic problems. While HYSPLIT back trajectories do not guarantee pure  
101 end members were sampled, the air masses were dominated by either North African or European  
102 origins. Ambient aerosol samples were stored at -20°C until analysis.

## 103 **2.2 Emission source collection**

104 Emissions from ultra-low sulfur diesel fuel and gasoline were collected using US  
105 Environmental Protection Agency protocols under typical urban driving conditions [Oakes *et al.*,  
106 2012b]. Coal fly ash from an electrostatic precipitator, provided by The Southern Company, was  
107 aerosolized and collected with a PM2.5 cyclone inlet sampler [Oakes *et al.*, 2012b]. Smoke  
108 produced from the burning of materials collected from coniferous and deciduous trees native to  
109 Georgia, USA, was sampled during a controlled biomass burning experiment using a cyclone  
110 inlet sampler placed 3.5 m above the burn area at a flow rate of 16.7 L min<sup>-1</sup> for approximately  
111 30 minutes. The ash produced from the biomass burning experiment was also analyzed.  
112 Although emission sources were not collected from European or North African locations, source  
113 materials presented here are considered to be reasonably similar to those found in Europe and  
114 North Africa. Thus, these emission sources can be used as a proxy for primary phosphorus  
115 sources found in European and North African air masses. In addition to the above emission  
116 sources, the following commercially available source materials were analyzed: pollen (*Quercus*

117 *ruba*; Sigma P7895), the bacteria *Azotobacter vinelandii* (Sigma A2135), and the bacteria  
118 *Bacillus subtilis* (Sigma B4006). This commercially available material was handled and analyzed  
119 in the same manner as phosphorus standards (Supporting Material). Emission source samples  
120 were stored at -20°C until analysis.

121 **2.3 Total phosphorus and soluble phosphate determination**

122 Total phosphorus was measured for all samples with a technique employing high temperature  
123 combustion (550°C for 2 hours) followed by extraction in acid (1N HCl, agitated for 24 hours)  
124 [Aspila *et al.*, 1976]. The extracts were centrifuged prior to analysis to remove suspended  
125 particles. Total phosphorus content was measured using standard spectrophotometric techniques  
126 [Murphy and Riley, 1962]. Soluble phosphate was determined for all samples collected at the  
127 Finokalia research station. For these samples half of a Teflon filter was extracted by sonicating  
128 with 15 ml of nanopure water (Milli-Q, resistivity: 18.2 MΩ-cm) for 45 minutes. Prior to  
129 analysis, each extracted solution was filtered through polyethersulfone membrane (PES) filters  
130 (0.45 µm pore size diameter), to remove suspended particles. A Dionex AS4A-SC column with  
131 ASRS-ULTRA-II suppressor in autosuppression mode of operation was used for the analysis of  
132 dissolved inorganic phosphate (DIP). The reproducibility of the measurements defined as  
133 standard deviation of five consecutive analyses was better than 2%. The detection limit, defined  
134 as 3 times the standard deviation of the blank, was 0.06 µM DIP.

135 **2.4 Synchrotron-based X-ray spectromicroscopy**

136 Samples were analyzed on the X-ray fluorescence microscope located at beamline 2-ID-B at  
137 the Advanced Photon Source, Argonne National Laboratory. The beamline is optimized to  
138 examine samples over a 1-4 keV energy range using a focused X-ray beam with a spot size of  
139 approximately 100 nm<sup>2</sup>[McNulty *et al.*, 2003]. Phosphorus Near Edge X-ray Fluorescence

140 Spectroscopy (P-NEXFS) data were collected in two modes that differ based on spatial  
141 resolution. In the first mode, individual phosphorus-rich particles with a diameter of greater than  
142 1 micron identified in X-ray fluorescence maps; these particles were then interrogated with  
143 micro P-NEXFS. The individual phosphorus-rich particles seen in X-ray fluorescence maps are  
144 obvious contributors to total sample phosphorus. However, much of the total phosphorus on an  
145 aerosol filter can also be contained in particles that are less phosphorus-rich and therefore less  
146 apparent in X-ray fluorescence maps. Therefore, in the second mode, large areas of the filters  
147 were also examined with an unfocused beam (spot size =  $0.28\text{ mm}^2$ ) to obtain bulk spectra  
148 representative of the average phosphorus phase present.

149 In order to maximize the number of samples analyzed in the allotted time, X-ray fluorescence  
150 maps were created by rastering the focused beam in  $0.5\text{ }\mu\text{m}$  steps with an incident energy of  
151 2185 eV. At this resolution, individual phosphorus-rich particles were clearly discernable.  
152 P-NEXFS spectra were collected over an energy range of 2130 to 2210 eV in 0.33 eV steps,  
153 using a 1 s dwell time at each step. Each P-NEXFS measurements for both bulk and individual  
154 phosphorus-rich particles were repeated at least three times, in a single position, creating a  
155 minimum effective dwell time of 3 s. X-ray spectromicroscopy data were collected using an  
156 energy dispersive silicon drift detector (Ketek with a  $5\text{ mm}^2$  sensitive area). A flow of helium  
157 was introduced between the X-ray optical hardware and the sample to reduce X-ray backscatter.  
158 An in-line monitor stick composed of fluorapatite was measured with each sample in order to  
159 identify and correct for any potential drift in monochrometer energy calibration that occurred  
160 during analyses [*de Jonge et al.*, 2010]. Clean areas of Teflon and cellulose acetate filters were  
161 examined as blanks and showed negligible background signal.

162 P-NEXFS provides essentially the same information as another commonly cited technique,  
163 P-XANES (X-ray Absorption Near Edge Structure) spectroscopy. The two techniques differ  
164 primarily in the method of signal detection. P-NEXFS uses the X-ray fluorescence signal which is  
165 inversely proportional to the absorption signal used in a XANES measurement.

166 **2.5 P-NEXFS data analysis**

167 Linear combination fitting is an effective tool for the deconvolution of spectra of known  
168 mixtures [Ajiboye *et al.*, 2007]. Using Athena software [Ravel and Newville, 2005], individual  
169 particle and bulk P-NEXFS spectra were fit with characterized phosphorus standard materials  
170 using the linear combination approach to determine both speciation and relative abundance of  
171 phosphorus phases [Prietzl *et al.*, 2013]. Additionally, bulk P-NEXFS spectra of ambient  
172 aerosol were fit using emission sources rather than standards; this approach was used to  
173 determine if phosphorus in ambient aerosol could be accounted for solely by emission sources.  
174 Athena used a non-linear, least-squares minimization approach to fit spectra of unknown  
175 materials with spectra of standard materials and computes an error term, R-factor, to quantify the  
176 goodness of fit produced by a particular linear combination of standard P-NEXFS spectra. The  
177 linear combination of standards that yielded the lowest R-factor reflected the best fit [Ravel and  
178 Newville, 2005].

179 The data for an individual P-NEXFS spectrum was normalized to create a relative intensity  
180 value of approximately 1 for post edge area of the spectra (> 2160 eV). The data were also  
181 processed using a three-point smoothing algorithm built into the software. Smoothing did not  
182 appreciably change the data, other than removing high frequency noise. The standard database  
183 used in our spectral linear combination fitting included phosphorus minerals and inorganic  
184 phosphorus compounds discussed in Ingall *et al.* 2011, as well as a variety of organic phosphorus

185 compounds (Supporting Material). An iterative process was used to refine the standard database  
186 used to model the sample spectra. First, complex, high temperature, and high-pressure minerals,  
187 unlikely to be major components of aerosol phosphorus were excluded from the database [Oakes  
188 *et al.*, 2012a]. Second, the database was narrowed through elimination of standards with low  
189 contribution (i.e. less than 10%) or poor fit (i.e. high R-factor) during initial linear combination  
190 fitting. Finally, the composition of individual phosphorus-rich particles determined using micro  
191 P-NEXFS helped to guide the choice of standards for the modeling of bulk P-NEXFS spectra.

192 Spectra can be very similar within certain compound classes like phosphorus esters  
193 (Figure S2) and mineral classes like apatites [Ingall *et al.*, 2011]. Also, insufficient quantities of  
194 a specific mineral or compound in a sample can also lead to underestimation of the specific  
195 compound during linear combination fitting [Hesterberg, 2010]. We therefore generalized our  
196 results into four chemical classes, apatite, metal phosphates, alkali and alkaline earth metal  
197 phosphates, and organic phosphorus + polyphosphate, with distinct implications for phosphorus  
198 solubility and bioavailability. The apatite chemical class includes fluorapatite, hydroxyapatite,  
199 carbonate fluorapatite and carbonate hydroxyapatite and chlorapatite. Minerals in the metal  
200 phosphate chemical class have a dominant metal cation like iron, copper, or manganese and  
201 include vauxite, cornetite, wardite, and wolfeite. Alkali and alkaline earth metal phosphates  
202 (hereafter referred to as alkali phosphates) include sodium phosphate and calcium dihydrogen  
203 phosphate; these phases typically have high solubility. The final chemical class, organic  
204 phosphorus + polyphosphate, includes organic compounds like adenosine-5'-triphosphate (ATP),  
205 lipids (and other phosphorus esters), and polyphosphates, all compounds of biological origin.

206

207

208 **3. Results and Discussion**

209 **3.1 Ambient aerosols**

210       Aerosol phosphorus from North African air masses was on average  $15.5 \pm 14.1\%$  soluble. In  
211 contrast, aerosol phosphorus from European air masses was on average  $54.0 \pm 5.6\%$  soluble  
212 (Figure 1). Despite European-sourced aerosols having less total phosphorus than North African  
213 aerosols, the mass of soluble phosphorus per mass of aerosol is comparable (Figure 1).  
214 Consistent with our findings based on our limited sample set, sequential extraction methods have  
215 shown that anthropogenically-influenced air masses, such as those originating in Europe, tend to  
216 have more soluble phosphorus than North African aerosol [Anderson *et al.*, 2010; Izquierdo *et*  
217 *al.*, 2012]. Our bulk P-NEXFS measurements further showed that European-sourced aerosols  
218 were dominated by the organic phosphorus + polyphosphate chemical class and were on average  
219 composed of  $93.8 \pm 13.9\%$  organic phosphorus + polyphosphate and  $6.2 \pm 13.9\%$  metal  
220 phosphate, with no alkali phosphates or apatite (Figure 2). In contrast, the average phosphorus  
221 composition of North African-sourced aerosols was  $32.3 \pm 33.2\%$  apatite,  $24.9 \pm 29.5\%$  alkali  
222 phosphates,  $24.8 \pm 26.9\%$  organic phosphorus + polyphosphate, and  $18.1 \pm 27.2\%$  metal  
223 phosphate (Figure 2). Micro P-NEXFS analysis revealed that individual phosphorus-rich  
224 particles from European and North African air masses were often solely comprised of organic  
225 phosphorus + polyphosphate or apatite, respectively.

226       Previous studies based on sequential extraction techniques have shown that apatite is the  
227 most abundant phosphorus phase followed by oxide-associated phosphorus in North African-  
228 sourced air masses [Anderson *et al.*, 2010; Nenes *et al.*, 2011]. Our results suggest  
229 organic phosphorus + polyphosphate as well as alkali phosphates account for a large fraction of  
230 the phosphorus in the North African derived aerosol (Figure 2). The oxide-associated phosphorus

fraction determined by sequential extraction techniques can include labile organic phosphorus as well [Anderson *et al.*, 2010]. Therefore, our finding of organic phosphorus + polyphosphate in North African-sourced aerosols could be consistent with extraction studies and suggest organic phosphorus is present in the oxide-associated fraction identified in these studies. The presence of alkali phosphates in North African air masses may reflect recycling of apatite-derived phosphorus. At low pH, apatite more readily dissolves into aerosol water droplets [Anderson *et al.*, 2010] that are subsequently dehydrated, possibly resulting in supersaturation of these droplets with respect to alkali phosphates. If sulfuric acid is the dominant acidic species present, aerosol water content may continue to be high even at low pH, which further facilitates dissolution of phosphorus.

Soluble phosphorus percentage shows the strongest correlation with the relative abundance of organic phosphorus + polyphosphate (Figure 3). However, the correlation coefficient of 0.61 indicates that significant variability in this relation exists. Solubility is likely tied to the abundance of specific organic phosphorus compounds *within* the defined chemical class. Organic phosphorus compounds exhibit a wide range of structures and compositions that are generally not possible to distinguish with P-NEXFS (Supporting Material). These species, in turn, differ in terms of phosphorus solubility. Also, acidification of normally insoluble phosphorus phases can increase phosphorus solubility [Nenes *et al.*, 2011]. Anthropogenic emissions are well-documented sources of acidic species [Nenes *et al.*, 2011] and have also been linked to more soluble forms of aerosol phosphorus [Izquierdo *et al.*, 2012; Zamora *et al.*, 2013]. Varying quantities of acidic species [Nenes *et al.*, 2011] entrained in European and North African air masses would likely lead to different levels of phosphorus solubilization during atmospheric transport.

254 **3.2 Emission Sources**

255 In addition to ambient aerosol samples, several common emission sources were analyzed  
256 with bulk P-NEXFS. Spectral linear combination fitting showed that pollen and the bacteria  
257 *Bacillus subtilis* and *Azotobacter vinelandii* were dominated by organic phosphorus +  
258 polyphosphate. Coal fly ash, diesel, volcanic ash, and biomass burning ash were comprised of  
259 apatite, metal phosphates and organic phosphorus + polyphosphate. Neither gasoline nor biomass  
260 burning emissions showed a discernable phosphorus edge, so phosphorus composition could not  
261 be characterized for these sources. Spectral linear combination fits based only on source  
262 emission spectra for ambient aerosol samples were usually inferior to fits utilizing phosphorus  
263 compounds and minerals. The dissimilarity between source emissions and ambient aerosol  
264 suggest either that atmospheric processing strongly modifies phosphorus composition or that  
265 another unknown phosphorus source is a dominant aerosol component. For example, aerosol  
266 production by plants and other organisms is a possible source of organic aerosol phosphorus  
267 [Artaxo *et al.*, 2002; Benitez-Nelson, 2000]. Biogenic pathways involved in aerosol production  
268 remain uncertain [Artaxo *et al.*, 2002; Benitez-Nelson, 2000]; however, primary emissions from  
269 vegetative cover could also account for the dominance of organic phosphorus + polyphosphate  
270 class seen in European air masses. Microbial cells have also been recognized as an important  
271 natural component of aerosol [Bauer *et al.*, 2002; Burrows *et al.*, 2009]. Due to a globally  
272 ubiquitous distribution[Bauer *et al.*, 2002; Burrows *et al.*, 2009], bacteria are potentially a key  
273 contributor to the organic fractions present in both the North African and European aerosol  
274 examined here. In fact, when emission sources were used as standards in spectral linear  
275 combination fitting, fits containing bacteria as a standard, produced the best results for both  
276 ambient aerosols sampled from North African and European air masses.

277

278 **4. Conclusions**

279 This work demonstrates, based on our limited data set, that synchrotron-based techniques  
280 provide valuable insights into the composition and therefore the factors influencing the solubility  
281 and bioavailability of phosphorus in aerosols. The distinctively higher phosphorus solubility in  
282 European aerosol is attributed largely to the presence of organic phosphorus. Preliminary  
283 evidence suggests that this organic phosphorus may be associated with bacteria; however, further  
284 research is necessary to specifically characterize the organic phosphorus containing phases and  
285 determine the prevalence of bacteria in Mediterranean aerosols. Shifts in wind direction observed  
286 over seasonal and inter-annual timescales [Chamard *et al.*, 2003] have been suggested as a key  
287 factor controlling the delivery of vital nutrients to marine systems [Hamza *et al.*, 2011]. Climate  
288 simulations suggest that European-sourced winds will be more prevalent over the Mediterranean  
289 Sea than North African-sourced winds in the future [McInnes *et al.*, 2011]. If phosphorus in  
290 European aerosol is consistently shown to be 3.5 times more soluble than North African aerosol,  
291 the increased European influences will lead to more soluble phosphorus loading to the  
292 Mediterranean Sea and ultimately more biological productivity.

293

294

295

296 **Acknowledgments.** This material is based upon work supported by the National Science  
297 Foundation under Grant OCE 1060884. Any opinions, findings, and conclusions or  
298 recommendations expressed in this material are those of the authors and do not necessarily  
299 reflect the views of the National Science Foundation. Use of the Advanced Photon Source is  
300 supported by the U.S. Department of Energy, Office of Basic Energy Sciences under contract  
301 No. DE-AC02-06CH11357. NM and KV acknowledge support from European Union (European  
302 Social Fund) and Greek national funds through the Operational Program "Education and  
303 Lifelong Learning" of the National Strategic Reference Framework Research Funding Program,  
304 ARISTEIA. We thank John Jansen at Southern Co. and Bill Preston at the EPA for providing  
305 source emission samples. Finally, we thank Terry Lathem for the volcanic ash sample.

306

307 **References**

309 Ajiboye, B., O. O. Akinremi, and A. Jurgensen (2007), Experimental validation of quantitative XANES analysis for  
310 phosphorus speciation, *Soil Science Society of America Journal*, 71(4), 1288-1291.

311 Anderson, L. D., K. L. Faul, and A. Paytan (2010), Phosphorus associations in aerosols: What can they tell us about  
312 P bioavailability?, *Mar. Chem.*, 120(1-4), 44-56.

313 Artaxo, P., J. V. Martins, M. A. Yamasoe, A. S. Procopio, T. M. Pauliquevis, M. O. Andreae, P. Guyon, L. V. Gatti,  
314 and A. M. C. Leal (2002), Physical and chemical properties of aerosols in the wet and dry seasons in Rondonia,  
315 Amazonia, *Journal of Geophysical Research-Atmospheres*, 107(D20).

316 Aspila, K. I., H. Agemian, and A. S. Y. Chau (1976), A semi-automated method for the determination of inorganic,  
317 organic and total phosphate in sediments., *Analyst*, 101, 187-197.

318 Baker, A. R., T. D. Jickells, M. Witt, and K. L. Linge (2006), Trends in the solubility of iron, aluminium,  
319 manganese and phosphorus in aerosol collected over the Atlantic Ocean, *Mar. Chem.*, 98(1), 43-58.

320 Bauer, H., A. Kasper-Giebl, M. Loflund, H. Giebl, R. Hitzenberger, F. Zibuschka, and H. Puxbaum (2002), The  
321 contribution of bacteria and fungal spores to the organic carbon content of cloud water, precipitation and aerosols,  
322 *Atmospheric Research*, 64(1-4), 109-119.

323 Beauchemin, S., D. Hesterberg, J. Chou, M. Beauchemin, R. R. Simard, and D. E. Sayers (2003), Speciation of  
324 phosphorus in phosphorus-enriched agricultural soils using X-ray absorption near-edge structure spectroscopy and  
325 chemical fractionation, *Journal Of Environmental Quality*, 32(5), 1809-1819.

326 Benitez-Nelson, C. R. (2000), The biogeochemical cycling of phosphorus in marine systems, *Earth-Science  
327 Reviews*, 51(1-4), 109-135.

328 Burrows, S. M., W. Elbert, M. G. Lawrence, and U. Poschl (2009), Bacteria in the global atmosphere - Part 1:  
329 Review and synthesis of literature data for different ecosystems, *Atmospheric Chemistry and Physics*, 9(23), 9263-  
330 9280.

331 Chamard, P., F. Thiery, A. Di Sarra, L. Ciattaglia, L. De Silvestri, P. Grigioni, F. Monteleone, and S. Piacentino  
332 (2003), Interannual variability of atmospheric CO<sub>2</sub> in the Mediterranean: measurements at the island of  
333 Lampedusa, *Tellus Series B-Chemical and Physical Meteorology*, 55(2), 83-93.

334 Chen, H. Y., T. H. Fang, M. R. Preston, and S. Lin (2006), Characterization of phosphorus in the aerosol of a coastal  
335 atmosphere: Using a sequential extraction method, *Atmospheric Environment*, 40(2), 279-289.

336 de Jonge, M. D., D. Paterson, I. McNulty, C. Rau, J. A. Brandes, and E. Ingall (2010), An energy and intensity  
337 monitor for X-ray absorption near-edge structure measurements, *Nuclear Instruments & Methods in Physics  
338 Research Section a-Accelerators Spectrometers Detectors and Associated Equipment*, 619(1-3), 154-156.

339 Draxler, R. R., and G. D. Hess (1998), An overview of the HYSPLIT\_4 modelling system for trajectories, dispersion  
340 and deposition, *Australian Meteorological Magazine*, 47(4), 295-308.

341 Escudero, M., A. F. Stein, R. R. Draxler, X. Querol, A. Alastuey, S. Castillo, and A. Avila (2011), Source  
342 apportionment for African dust outbreaks over the Western Mediterranean using the HYSPLIT model, *Atmospheric  
343 Research*, 99(3-4), 518-527.

344 Ganor, E., and Y. Mamane (1982), Transport of Saharan dust across the Eastern Mediterranean, *Atmospheric  
345 Environment*, 16(3), 581-587.

346 Graham, W. F., and R. A. Duce (1982), The atmospheric transport of phosphorus to the western North-Atlantic,  
347 *Atmospheric Environment*, 16(5), 1089-1097.

348 Guerzoni, S., et al. (1999), The role of atmospheric deposition in the biogeochemistry of the Mediterranean Sea,  
349 *Progress in Oceanography*, 44(1-3), 147-190.

350 Hamza, W., M. R. Enan, H. Al-Hassini, J. B. Stuut, and D. de-Beer (2011), Dust storms over the Arabian Gulf: a  
351 possible indicator of climate changes consequences, *Aquatic Ecosystem Health & Management*, 14(3), 260-268.

352 Hesterberg, D. (2010), Chapter 11 - Macroscale Chemical Properties and X-Ray Absorption Spectroscopy of Soil  
353 Phosphorus, in *Developments in Soil Science*, edited by S. Balwant and G. Markus, pp. 313-356, Elsevier.

354 Ingall, E., J. Brandes, J. Diaz, M. de Jonge, D. Paterson, I. McNulty, W. Elliott, and P. Northrup (2011), Phosphorus  
355 K-edge XANES spectroscopy of mineral standards, *Journal of Synchrotron Radiation*, 18, 189-197.

356 Izquierdo, R., C. R. Benitez-Nelson, P. Masque, S. Castillo, A. Alastuey, and A. Avila (2012), Atmospheric  
357 phosphorus deposition in a near-coastal rural site in the NE Iberian Peninsula and its role in marine productivity,  
358 *Atmospheric Environment*, 49, 361-370.

359 Kalivitis, N., E. Gerasopoulos, M. Vrekoussis, G. Kouvarakis, N. Kubilay, N. Hatzianastassiou, I. Vardavas, and N.  
360 Mihalopoulos (2007), Dust transport over the eastern Mediterranean derived from Total Ozone Mapping

361 Spectrometer, Aerosol Robotic Network, and surface measurements, *Journal of Geophysical Research-Atmospheres*, 112(D3).

362 Kouvarakis, G., N. Mihalopoulos, A. Tselepidis, and S. Stavrakaki (2001), On the importance of atmospheric inputs  
363 of inorganic nitrogen species on the productivity of the eastern Mediterranean Sea, *Global Biogeochemical Cycles*,  
364 15(4), 805-817.

365 Krom, M. D., K. C. Emeis, and P. Van Cappellen (2010), Why is the Eastern Mediterranean phosphorus limited?,  
366 *Progress in Oceanography*, 85(3-4), 236-244.

367 Krom, M. D., N. Kress, S. Brenner, and L. I. Gordon (1991), PHOSPHORUS LIMITATION OF PRIMARY  
368 PRODUCTIVITY IN THE EASTERN MEDITERRANEAN-SEA, *Limnol. Oceanogr.*, 36(3), 424-432.

369 Mackey, K. R. M., K. Roberts, M. W. Lomas, M. A. Saito, A. F. Post, and A. Paytan (2012), Enhanced Solubility  
370 and Ecological Impact of Atmospheric Phosphorus Deposition upon Extended Seawater Exposure, *Environmental  
371 Science & Technology*, 46(19), 10438-10446.

372 Mahowald, N., et al. (2008), Global distribution of atmospheric phosphorus sources, concentrations and deposition  
373 rates, and anthropogenic impacts, *Global Biogeochemical Cycles*, 22(4).

374 Markaki, Z., K. Oikonomou, M. Kocak, G. Kouvarakis, A. Chaniotaki, N. Kubilay, and N. Mihalopoulos (2003),  
375 Atmospheric deposition of inorganic phosphorus in the Levantine Basin, eastern Mediterranean: Spatial and  
376 temporal variability and its role in seawater productivity, *Limnology and Oceanography*, 48(4), 1557-1568.

377 McInnes, K. L., T. A. Erwin, and J. M. Bathols (2011), Global Climate Model projected changes in 10 m wind  
378 speed and direction due to anthropogenic climate change, *Atmos Sci Lett*, 12(4), 325-333.

379 McNulty, I., et al. (2003), The 2-ID-B intermediate-energy scanning X-ray microscope at the APS, *Journal De  
380 Physique Iv*, 104, 11-15.

381 Murphy, J., and J. P. Riley (1962), A modified single solution method for the determination of phosphate in natural  
382 waters, *Analyt. Chim. Acta*, 27, 31-36.

383 Nenes, A., M. D. Krom, N. Mihalopoulos, P. Van Cappellen, Z. Shi, A. Bougiatioti, P. Zarmpas, and B. Herut  
384 (2011), Atmospheric acidification of mineral aerosols: a source of bioavailable phosphorus for the oceans,  
385 *Atmospheric Chemistry and Physics*, 11(13), 6265-6272.

386 Oakes, M., R. J. Weber, B. Lai, A. Russell, and E. D. Ingall (2012a), Characterization of iron speciation in urban  
387 and rural single particles using XANES spectroscopy and micro X-ray fluorescence measurements: investigating the  
388 relationship between speciation and fractional iron solubility, *Atmospheric Chemistry and Physics*, 12(2), 745-756.

389 Oakes, M., E. D. Ingall, B. Lai, M. M. Shafer, M. D. Hays, Z. G. Liu, A. G. Russell, and R. J. Weber (2012b), Iron  
390 Solubility Related to Particle Sulfur Content in Source Emission and Ambient Fine Particles, *Environmental Science  
391 & Technology*, 46(12), 6637-6644.

392 Prietzel, J., A. Dümig, Y. Wu, J. Zhou, and W. Klysubun (2013), Synchrotron-based P K-edge XANES  
393 spectroscopy reveals rapid changes of phosphorus speciation in the topsoil of two glacier foreland chronosequences,  
394 *Geochimica Et Cosmochimica Acta*, 108(0), 154-171.

395 Ravel, B., and M. Newville (2005), ATHENA, ARTEMIS, HEPHAESTUS: data analysis for X-ray absorption  
396 spectroscopy using IFEFFIT, *Journal of Synchrotron Radiation*, 12, 537-541.

397 Ridame, C., and C. Guieu (2002), Saharan input of phosphate to the oligotrophic water of the open western  
398 Mediterranean Sea, *Limnology and Oceanography*, 47(3), 856-869.

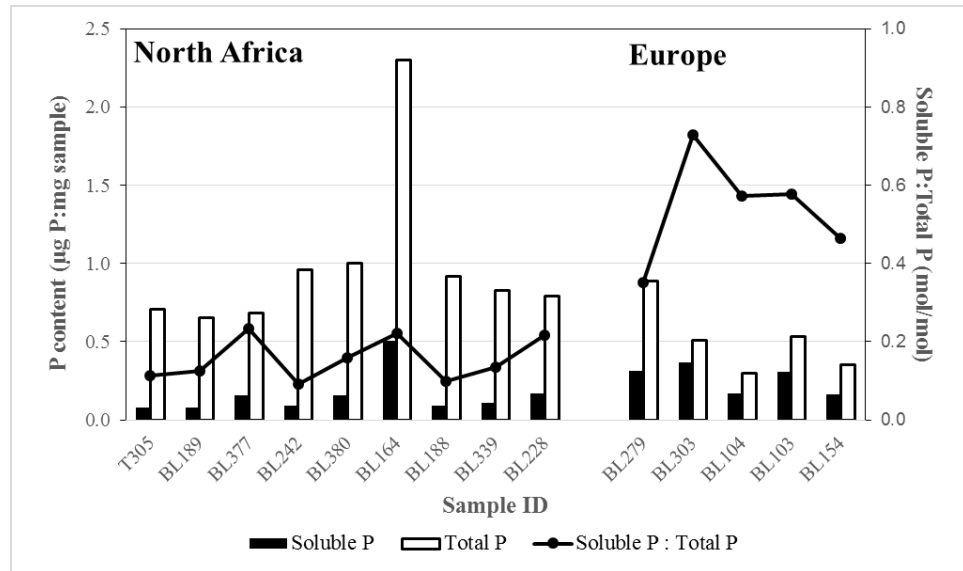
399 Zamora, L. M., J. M. Prospero, D. A. Hansell, and J. M. Trapp (2013), Atmospheric P deposition to the subtropical  
400 North Atlantic: sources, properties, and relationship to N deposition, *Journal of Geophysical Research-Atmospheres*,  
401 118(3), 1546-1562.

402

403

404

405

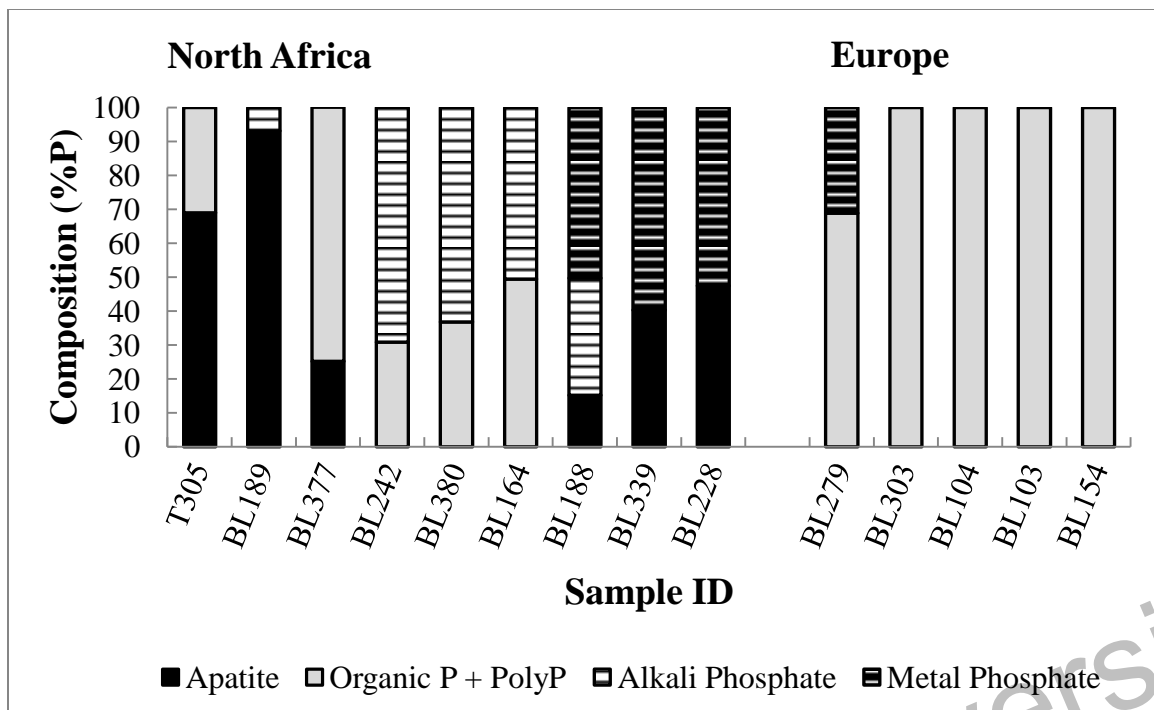


406

407 **Figure 1.** The soluble and total phosphorus contained in Mediterranean aerosols are shown for  
 408 air masses originating in Europe and North Africa. Total phosphorus content (white) and soluble  
 409 phosphorus content (black) show both European and North African samples are potential sources  
 410 of phosphorus to the Mediterranean Sea. The molar ratio of soluble phosphorus to total  
 411 phosphorus (line) expressed as a percentage shows European aerosol can be up to 4.7 times more  
 412 soluble than North African aerosol. Typically, the reproducibility for measuring soluble  
 413 phosphorus and total phosphorus are 2% and 10%, respectively.

414

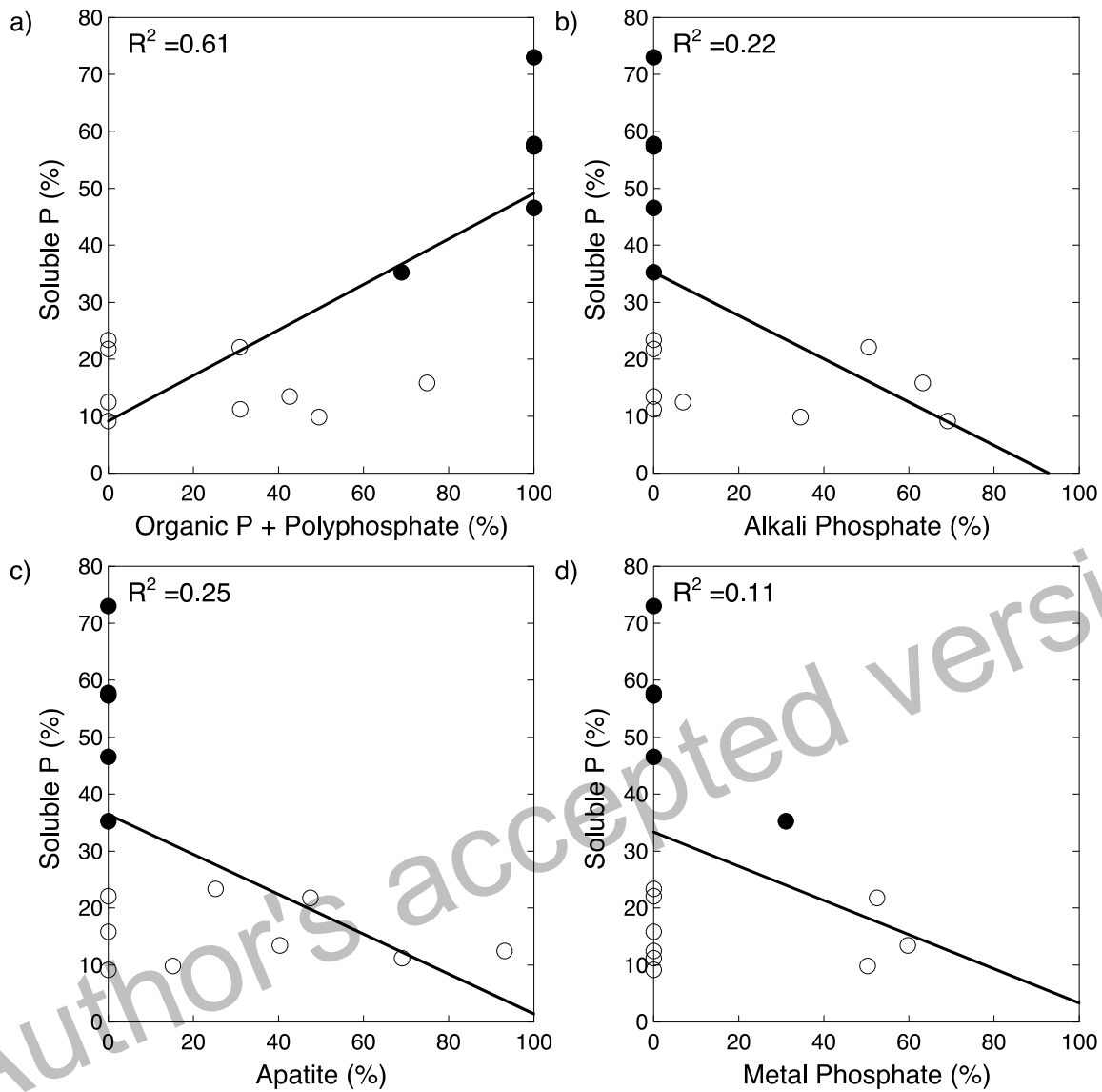
415



416

417 **Figure 2.**Linear combination fitting of each aerosol spectra was used to determine the  
 418 phosphorus composition in each sample. The distribution of apatite (black),  
 419 organic phosphorus + polyphosphate (grey), alkali phosphates(white striped), and metal  
 420 phosphates (black striped) determined through linear combination fitting are shown for each  
 421 sample.

422



423

424

425 **Figure 3.** Plots of percent soluble phosphorus versus phosphorus composition are shown for  
 426 North African (○) and European (●) sourced aerosol samples. The only chemical class showing a  
 427 notable correlation with solubility is organic phosphorus + polyphosphate (a) suggesting that this  
 428 class does in part influence solubility.

429

430